~~Improvement of online monitoring technology based on the Berthelot reaction and long path absorption photometer for the measurement of ambient NH_3: Field applications in low-concentration environments~~ Colorimetric derivatization of ambient ammonia (NH_3) for detection by long path absorption photometry

Shasha Tian[a, b, 1], Kexin Zu[a, b, 1], Huabin Dong[a, b, *], Limin Zeng [a, b], Keding Lu [a, b], Qi Chen [a]

[a] State Key Joint Laboratory of Environmental Simulation and Pollution Control, College of Environmental Sciences and Engineering, Peking University, Beijing, 100871, China.

[b] International Joint laboratory for Regional pollution Control (IJRC), Peking University, Beijing, China

* Corresponding author: hbdong@pku.edu.cn

Abstract. In the last few decades, various techniques, including spectroscopic, mass spectrometric, chemiluminescence, and wet chemical methods~~wet chemical and mass spectrometric methods~~, had been developed and applied for the detection of gaseous ammonia (NH_3). We developed an online NH_3 monitoring system~~ (~~salicylic acid derivatization reaction and long path absorption photometer (SAC-LOPAP)~~SAC-LOPAP)~~. based on a selective colorimetric reaction to form a highly absorbing reaction product ~~Berthelot reactions~~ and a ~~long path absorption photometer (~~LOPAP~~)~~, which could run stably ~~run statically~~ for a long time and be applied to the continuous online measurement of low concentrations of ambient ~~air~~NH_3 by optimizing the reaction conditions, adding a constant temperature module and liquid flow controller. The detection limit reached with this instrument was 40.5 ppt with a stripping liquid flow rate of 0.49 ml min^{-1} and a gas sample flow rate of 0.70 L min^{-1}~~under stable conditions~~. ~~In addition, the range of NH_3 measurement varied from background contamination (<40.5 ppt) to approximately 100 ppb in the current condition (a stripping liquid flow rate of 0.49 ml min^{-1} and a gas sample flow rate of 0.70 L min^{-1}).~~ An inter-comparison of our system with ~~a~~ a commercial instrument Picarro G2103 analyzer (Picarro, US)~~another established system~~ in Beijing was presented, and the results showed that the two

instruments had a good correlation with a slope of 1.00 and an R^2 of 0.96, indicating that the SAC-LOPAP involved in this study could be used for the accurate measurement of NH_3.

1. Introduction

Gaseous ammonia (NH_3) widely exists in the atmosphere and plays an important role in many atmospheric chemical reactions (Swati and Hait, 2018; Klimczyk et al., 2021; Wang et al., 2018). As the most abundant alkaline gas in the atmosphere, NH_3 easily forms ammonium ions (NH_4^+) with water and reacts with acidic species to form secondary inorganic particles ~~ acid~~ (Ianniello et al., 2011; Ni et al., 2000)~~. precursors such as SO_2 and NOx ($NO+NO_2$) to generate secondary aerosols,~~ These secondary particles are considered a major source of fine particulate matter (PM), which is harmful to climate, visibility and human health (Wang et al., 2015). Furthermore, recent studies have shown that NH_3 is necessary to control fine particulate pollution (Wen et al., 2018; Wang et al., 2013). Due to those problems, the inventory of NH_3 emissions and concentration in urban air has been highly evaluated. Agriculture, including animal feedlot operations, is considered as the largest emission source of NH_3 with 80.6% of the global anthropogenic emissions followed by 11% from biomass burning and 8.3% from the energy sector, including industries and traffic (Behera et al., 2013). Expert ~~Fowler et al.~~ estimate that global annual emissions of NH3 will increase from 65 Tg N yr^{-1} in 2008 to 135 Tg N yr^{-1} in 2100 (Fowler et al., 2015). However, ambient measurement of NH_3 concentrations is difficult due to several factors: ambient levels vary widely with from 5 pptv to 500 ppbv (Janson et al., 2010; Krupa, 2003; Sutton et al., 1995). Ammonia exists in gaseous, particulate and liquid phases, which add further complicates the measurement (Warneck, 1988). In addition, NH_3 is "sticky" and interacts with surfaces of materials, resulting in slow inlet response times (Yokelson et al., 2003). Finally, the temperature difference between the indoor and outdoor environments and the humidity difference between the inside and outside of the instrument will reduce the accuracy of measurement and calibration.~~which have a significant impact on the generation of particulate matter (Baek and Aneja, 2004; Behera et al., 2013). Kirkby, j. et al. found that trace amounts of NH_3 (less than 100 ppt) could increase the nucleation rate of sulfate radicals by 2-10 times in a CLOUD experiment on the nucleation of new particles. B. Bessagnet et al. found that the estimation of ammonium particle formation was insufficient, arguing that the role of ammonium in PM was more significant than initially thought (Bessagnet et al., 2014). In recent decades,~~

~~the emissions of SO_2 and NOx have been controlled to some extent, but the emission reduction of NH_3 is less than that of SO_2 and NOx (Scab et al., 2020). Therefore, accurate measurement of NH_3 is essential for public health and to further reduce secondary aerosol generation.~~ It is therefore essential to accurately measure ambient NH_3 to better quantify concentration and concentration changes and hence to evaluate the impacts of NH_3.

~~There are several difficulties in detecting NH_3 in the atmosphere due to its strong adsorption and hygroscopicity. The adsorption and hygroscopic properties of NH_3 are caused by the formation of a strong hydrogen bond between water and NH_3 (Hüglin, 2004). Due to the character of NH_3, it can readily be adsorbed on the surface of the sampling tube, resulting in~~ (Yokelson and R., 2003)~~low measurements and slow response. In particular, NH_3 is likely to be adsorbed on the metal surface of optical systems in the spectrometric monitoring instrument, resulting in increased background . In addition, the temperature difference between the indoor and outdoor environments and the humidity difference between the inside and outside of the instrument will reduce the accuracy of measurement and calibration.~~

In recent years, researchers have developed techniques and methods for detecting NH_3 in the atmosphere, which include spectroscopic, mass spectrometric, chemiluminescence, and wet chemical methods ~~wet chemical and mass spectrometric methods~~ (Von et al., 2009). Spectroscopic methods, such as Cavity Enhanced Absorption Spectroscopy (CEAS) (Gong et al., 2017; Berden et al., 2000) and Cavity Ring-Down Spectroscopy (CRDS) (Martin et al., 2016; Qu et al., 2012), can greatly improve spectral absorption's effective optical path length by using the optical cavity structure. However, the "sticky" of NH_3 will affect ~~has a high viscosity and easily adheres to the metal surface of optical systems in spectrometric monitoring instruments, thus affecting the~~ background, detection efficiency and detection response time of the instrument (Whitehead et al., 2008; Yokelson et al., 2003). Utilizing a quantum cascade laser (QCL) or a DFB laser in a near-infrared band as the light source can achieve ~~high detection accuracy and~~ a low detection limit of 0.018ppb (Whitehead et al., 2008; Mcmanus et al., 2002; Von et al., 2009), realizing the measurement of low concentrations of NH_3 in ambient air. Mass-spectrography analyzers provide highly sensitive techniques but may be less specific and can be affected by competing ion chemistries. The chemical ionization mass spectrometer (CIMS) technique is based on an ion-molecule reaction to selectively ionize and detect trace NH_3 ~~species~~ in the atmosphere, which features a fast response and in situ measurement (Benson et al., 2010; Nowak et al., 2007; Yu and Lee, 2012). ~~he~~

sensor measurement method relies on the response of special materials to NH_3. It has the advantages of small volume and wide measurement range, but its detection limit is very high (Ajay and Beniwal., 2019). Chemiluminescence is an indirect method to measure ammonia. Two catalytic converters of different characteristics catalyze NOx and NO-amine into NO. The NH_3 mining ratio is calculated by the difference between NOx and NO-amine. This method can realize the simultaneous measurement of NH_3, NO and NO_2, but the measurement results are affected by the conversion efficiency (Sharma et al., 2010; Sharma et al., 2012). Wet chemistry methods convert gas-phase NH_3 to aqueous NH_3 (NH_4^+) for online analysis by means of online ion chromatography with a detection limit of 0.05 μg m^{-3} (0.72ppb at 25 ℃) (Khlystov et al., 1995; Dong et al., 2012; Makkonen et al., 2012). usually require a combination of a wet chemistry collection system and a wet chemistry analyzer, such as a dull-polished wet tubing denuder (WAD), which can separate gaseous NH_3 and aerosol particles. NH_3 is absorbed and ionized to NH_4^+ to be analyzed by ion chromatography (Dong et al., 2012). A field inter-comparison of NH_3 measurement techniques found that wet chemistry instruments showed better long-term stability and agreement than other analyzers (Von et al., 2009), which was due to the wet chemical trapping method and standard calibration solutions, humidity did not affect the measurement, and the standard solution was more stable than standard gases. However, they failed to capture the peak because of lower time resolution. Mass spectrography analyzers provide highly sensitive techniques but may be less specific and can be affected by competing ion chemistries. Furthermore, Based on a the selective colorimetric reaction to form a highly absorbing reaction productBerthelot reaction and absorption spectrophotometry collect NH_3 (and ammonium) by aqueous scrubbing in glass frit impactors (Bianchi et al., 2012; Bae et al., 2007),– has been used for decades for routine derivatization and colorimetric analysis of NH_4^+ in a wide variety of environmental samples (e.g. soils, environmental waters, etc), which is a new wet chemistry method for the determination of NH_3 that has also been reported by other scholars (Bae et al., 2007). In those studies the product was detected by a long- path absorption photometer (LOPAP), in which the absorbance of the solution is amplified in the long-l path module to reach a lower detection limit (Heland et al., 2001).

In this study, we provide an online NH_3 monitoring system based on wet chemistry stripping of atmospheric NH_3, followed by the formation of a highly light-absorbing indophenol after a salicylic acid derivatization reaction to produce the colored reaction product chromogenic reaction and detected with LOPAP. quantification of the reaction product by a home-made long-path absorption photometer

(LOPAP)According to Lambert-Beer's law, the sensitivity of spectrophotometry can be enhanced by increasing the optical path length. –This sensitive analytical method has already been successfully applied in different colorimetric detection studies (Yao et al., 1998; Heland et al., 2001; Callahan et al., 2002). In analogy to the original long path absorption photometer (LOPAP) which was developed for HONO measurements (Kleffmann et al., 2002), We we call this monitoring system the salicylic acid derivatization reaction chromogenic and long path absorption photometer (SAC-LOPAP), which features several improvements over versions previously reported by other groups: one is the optimization of reaction conditions, the other modification is the use of constant temperature module and flow control system. Secondly, we will present measurements demonstrating our new system in urban environments in Peking University, with measure low concentrations, good stability and low detection limit. The objective of this study is to optimize the key parameters based on the Berthelot reaction and absorption spectrophotometry, establish a method suitable for the instrument can run statically for a long time and can be used for the continuous online measurement of low concentrations ammonia of ambient air.

2. MethodsSAC-LOPAP instrument

2.1 Measurement principle

Our instrument is designed to measure NH_3 in a low-concentration environment (under 20ppb) with the good stability, low detection limit (less than 60 ppt) and small size. There is a brief introduction to the principle of the instrument. The measurement of NH_3 in the SAC-LOPAP instrument is achieved by the selective colorimetric reaction to form a highly absorbing reaction product and absorption spectrophotometryBerthelot reaction method. Samples containing dissolved ammonia and ammonium react with a phenolic compound and a chlorine-donating reagent to form indophenol blue during the reaction, with the strongest absorption at a wavelength of 665 nm. This reaction is more sensitive than other chromogenic reactions, such as reactions based on Nesslers's reagent (Krom and Michael, 1980; Searle and Phillip, 1984). Fig. 1 shows tThe reaction mechanism of the chromogenic reactions as shown in (1)-(4). Furthermore, to measure the absorbance of the sample, we used a LOPAP a long path absorption photometer (LOPAP) based on liquid-waveguide capillary cell (LWCC) technology to obtain a better detection limit, continuity and stability (Heland et al., 2001).

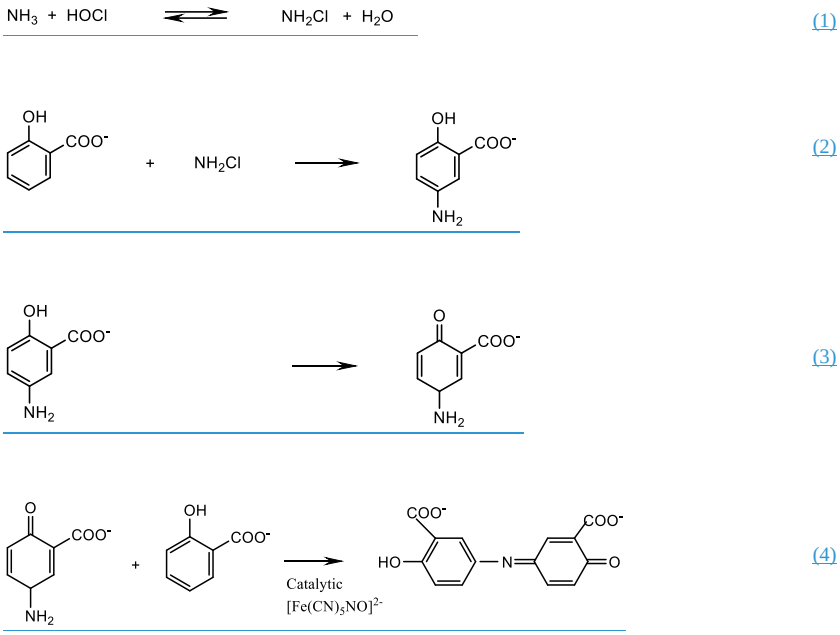

~~(Searle and Phillip, 1984)~~We acknowledge that Berthelot reactions must be carried out under ~~catalytic and alkaline conditions. $[Fe(CN)_5NO]^{2-}$ is recognized as a high efficiency catalytic to increase the sensitivity of the Berthelot reactions (Krom and Michael, 1980; Searle and Phillip, 1984). However, precipitates containing $Fe(OH)_3$ form during the reaction process, which comes from the reaction of $[Fe(CN)_5NO]^{2-}$ with NaOH. These precipitates have little effect on off-line instruments.~~

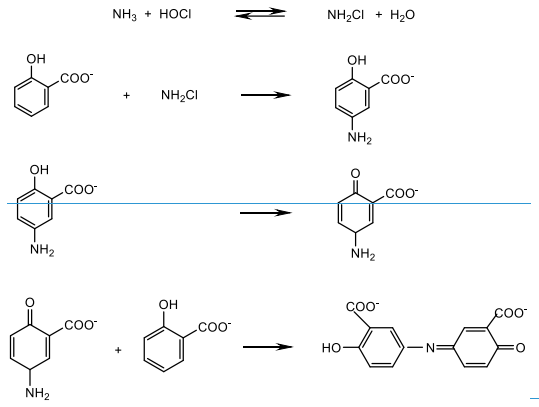

~~Fig. 1. The reaction mechanism of salicylic acid chromogenic reactions~~

2.2 Experiment setup

~~As shown in Fig. 2, w~~We designed our system to consist of four modules: the sampling module, the reacting module, the detecting module, and the control module (Fig. 1). The key component of the sampling module is a glass coil reactor, ~~The sampling module contains a~~which is an open glass tube (inner diameter 1.5 mm, 75 cm long) coiled 12 turns. At the beginning of this coil, there is a flow manifold to mix the ambient air flow and the stripping solutions. The air is pumped into the stripping coil under the action of a vacuum diaphragm air pump ~~(Nidec, Japan)~~ and a gas flow meter (Horiba, China) (Chen et al., 2004). To protect the gas flowmeter and the air pump, a security bottle is installed in front of the gas flowmeter to prevent the inflow of liquid. At the same time, the stripping solution, regulated by the liquid flow control system, is injected into the stripping coil to capture NH_3 ~~components~~ in the air and form a mixture of ammonium-salicylic acid. To achieve higher absorption efficiency, circulating cooling water with a temperature of 10-15 ℃ is provided outside the stripping coil. The center part of the reacting module is a reaction ~~kettle~~ coil and a debubble. The liquid sample is mixed with ~~an~~ the alkaline derivatization solution, and a derivatization reaction to produce the colored reaction product ~~chromogenic~~ reaction occurs in the heated reaction ~~kettle~~ coil~~,~~. The reaction coil ~~which~~ is made of a 90 cm length of Teflon tubes coiled on a heat-conducting metal cylinder, and ~~the~~ae ~~built-in heating rod and temperature sensor~~ PID controller controls the temperature of the reactor at 40-75 ℃ to accelerate the derivatization reaction. After the derivatization reaction~~chromogenic reaction~~, the sample is sent to the detecting module, which comprises a liquid waveguide capillary cell (LWCC-100, World Precision Instruments, USA) with optical path length of 100 cm, an LED light source with the mode at 665 nm (Ocean Optics) ~~,~~ and a phototube (S16008-33, HAMAMTSU, Japan)~~HR-UV-14, -~~ for the long path photometry detection. ~~and a photoelectric detector.~~ The sample solution to be tested is filtered by a 1.0 μm filter before passing through LWCC to avoid interference from components of the sample matrix/method reagents. ~~contamination by precipitates in the solution. All instrument functions are controlled by the control module, including an integrated circuit and a touch panel.~~ Both the fluid propulsion module and detection module can be computer controlled. ~~The optical path length of LWCC is 100 cm. The NH_4^+ standard solution was produced by the National Institute of Metrology, China.~~

Eq. (~~1~~5) can help ~~invert~~ convert the concentration of NH_4^+ solution $C_{NH_4^+}$ to the NH_3 concentration in the ~~gas~~ gaseous ~~production sample~~ C_{NH_3}.

$$C_{NH_3} = \frac{C_{NH_4^+} F_l R T}{M_{NH_3} F_g P \gamma} \quad (~~1~~5)$$

Where C_{NH_3} denotes the content of NH_3 in the air sample (ppb), P denotes atmospheric pressure (101.3 kPa), M_{NH_3} denotes the molar mass of ~~NH_3~~ (17 g/mol), R=8.314 Pa ~~m~~^{3} ~~mol~~$^{-1}$ ~~K~~$^{-1}$. T denotes the room temperature ~~in the stripping solution (the temperature of the cycling water, the unit is~~ K), F_l denotes the flow rate of stripping solution, F_g denotes the flow rate of sampling gas, γ denotes the capture efficiency of air NH_3 in the stripping solution ~~(~~a constant determined by laboratory).

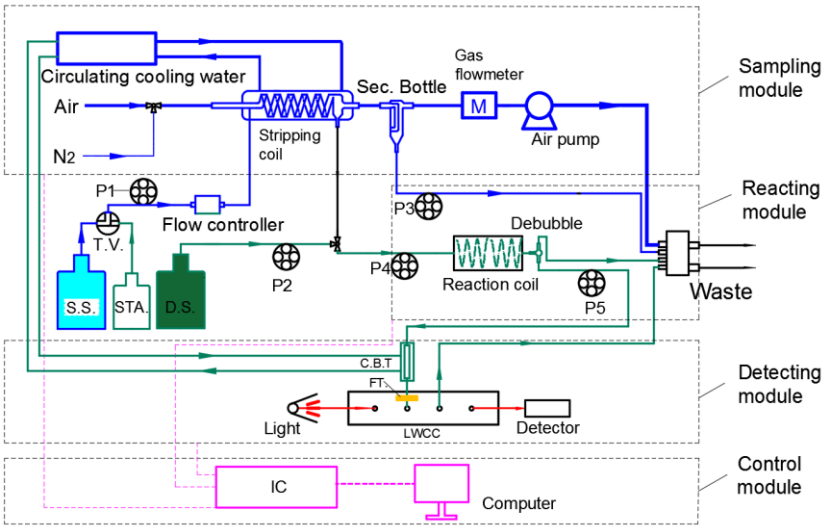

Fig. 1. Schematic diagram of SAC-LOPAP. (M: gas flowmeter; S.S.: stripping solution; STA.: standard solution; D.S.: derivatization solution; Sec. Bottle: security bottle; C.B.T: cooling buffer tube; T.V.: triple valve for switching stripping solution and standard solution; P1, P2, P3, P4, P5: peristaltic pump for transferring solutions; FT: syringe filter; IC: integrated circuit. The gas flow rate can be controlled from 0.2-2.0 L min^{-1}, with an optimal gas flow rate of 0.7 L min^{-1}. The liquid flow rate can be controlled from 0.1-1.0 ml min^{-1}, with an optimal stripping liquid flow rate of 0.49 ml min^{-1}).

~~2.3~~

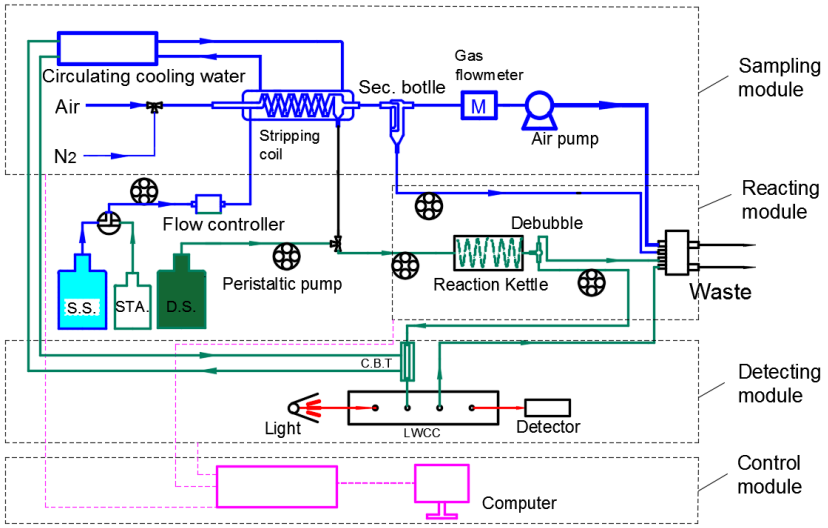

~~2.4~~

~~2.5 Fig. 2. Schematic diagram of SAC-LOPAP~~

2.3Experiment protocol

The exact recipe of the chemical reactions follows the reactions described by Searle et al (Searle and Phillip, 1984). We used 0.75g L^{-1} salicylic acid (TCI, 99.5%, Japan), 0.014 g L^{-1} sodium nitroferricyanide (TCI, 99%, Japan), and 0.2 g L^{-1} NaOH as stripping solution (R1). Then the 0.188ml L^{-1} Sodium hypochlorite (Aladdin, active chlorine10%, China) and 1.5 g L^{-1} NaOH as derivatization solution (R2). We acknowledge that based on a selective colorimetric reaction to form a highly absorbing reaction product must be carried out under catalytic and alkaline conditions. Sodium nitroferricyanide is recognized as a high-efficiency catalytic to increase the sensitivity of the Equation 4 (Krom and Michael, 1980; Searle and Phillip, 1984).

Calibrating the setup uses NH_4^+ standard solution produced by the National Institute of Metrology, China. The standards are prepared shortly before use by NH_4^+ standard solution with R1 in volumetric bottle and to use it right after it was ready. After replacement with new R1 and R2 solutions and other instrument fittings, the instrument should be recalibrated to ensure data quality.

2.4 Sampling method

The inter-comparison experiment was conducted at the College of Environment Sciences and Engineering, Peking University, located within the 4th ring road in northern Beijing, China (39.59 °N, 116.18 °E). A commercial instrument Picarro G2103 analyzer (Picarro, US) used for atmospheric NH_3 measurement based on the CRDS method was deployed concurrently with SAC-LOPAP in the comparison, which could be used to validate other instruments (Twigg et al., 2022). The experiment took place from 15 September 2021 to 15 October 2021, with the instruments installed in a field container. Two instruments shared an inlet and were deployed 2.5 m above the ground. A Polytetrafluoroethylene (PTFE) filter (46.2 mm diameter, 2 μm pore size, Whatman, USA) is used in the front of the sample module to remove ambient aerosols, which is placed into a round filter holder made of perfluoro alkoxy (PFA). We changed the filter every day with the aim of avoiding uncertainties. After the filtration of the aerosols, the sample gas flow is delivered into a 3.8 m long 1/4-inch Teflon tube, and a temperature-controlled metal heating wire (set at 35 ℃ ±0.1 ℃) is wrapped around the sample tube and covered with thermo-isolation materials. We ran our instrument with an additional drag flow of 1.75 L min^{-1} with aim to ensure the ambient residence time was about 7.8 msec for all instruments. Data acquisition times were different for the above instruments during the inter-comparison. The base reporting periods for Picarro and SAC-LOPAP were 1 s and 30 s. For the purposes of comparison, data from the two instruments presented in this section were averaged to 30 s. In addition, high purity N_2 as zero gas was injected into the sampling tube and carried out every 7 days at the start and end of the campaign as well. –The standard air source comes from China Sichuan Zhongce Biaowu Technology Co., LTD. The quality management system of the company conforms to the recognized standard in the Chinese industry (GB/T9001-2016/ISO 9001:2015). The composition was ammonia (5.08 ppm) and nitrogen with the uncertainty was 2%. In the test, pure N_2 was used as the dilution gas to obtain the required concentration of ammonia standard gas. Calibrations were performed using combinations of concentrations at 1.32, 4.95, 9.59, 17.90 and 54.96 ppb from the cylinder. In addition, 4.95 ppb and 54.96 ppb standard gas were injected into the sample tube every 7 days after zero point. The field container was controlled at 25 ℃ ±1 ℃ to reduce the impact of temperature fluctuations on measurement results.

3 Characterization and optimization

3.1 Sampling efficiency

NH_3 Standard gas of 54.96 ppb was used as the sample to be collected through two identical serial stripping coils, and the concentration of liquid samples collected by the two stripping coils was measured to calculate the capture efficiency. The calculation formula is as below.

$$\gamma_1 = \frac{c_1}{c_1+c_2} \times 100\% \quad (6)$$

Where, γ_1 denotes the collection efficiency of the first stripping coil, c_1 and c_2 denote the concentration of NH_4^+ trapped in the first stripping coil and the second stripping coil, respectively.

The collection efficiency of NH_3 from the R1 reached more than 99% under different c_{NaOH}, F_l, and F_g. Figure 2a and Figure 2b show that the F_l and the F_g had almost no influence on collection efficiency. Figure 2c shows that c_{NaOH} of 1.25 mmol L^{-1} achieved the greatest collection efficiency in the R1 (99.9%). Therefore, the c_{NaOH} of 1.25 mmol L^{-1} was selected as the R1 of the NH_3. And we selected F_l as 0.49 ml /min and F_g as 0.7 L min^{-1} in order to achieve the required detection range in this study.

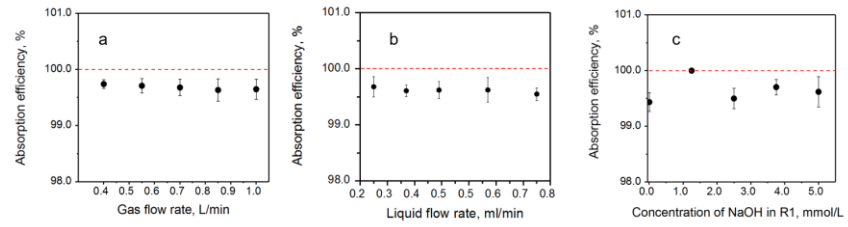

Fig. 2. The absorption efficiency of stripping coil versus (a) gas flow rate (c_{NaOH} = 4.0 mmol L^{-1}, F_l = 0.49 ml min^{-1}), (b) liquid flow rate (c_{NaOH} = 4.0 mmol L^{-1}, F_g = 0.7L min^{-1}), (c) concentration of NaOH in R1 (F_l = 0.49 ml min^{-1}, F_g = 0.7L min^{-1}).

~~3 Characterization and optimization~~

~~We acknowledge that Berthelot reactions must be carried out under catalytic and alkaline conditions. $[Fe(CN)_5NO]^{2-}$ is recognized as a high efficiency catalytic to increase the sensitivity of the Berthelot reactions (Krom and Michael, 1980; Searle and Phillip, 1984). However, precipitates containing $Fe(OH)_3$ form during the reaction process, which comes from the reaction of $[Fe(CN)_5NO]^{2-}$ with NaOH. These precipitates have little effect on off-line instruments. But for on-line instruments, precipitates can attach~~

~~to the wall of the pipeline and LWCC, which leads to pipeline blockage and baseline drift. Therefore, we need to optimize reaction conditions, add the constant temperature module and liquid flow controller temperature, and so on to achieve continuous online measurement of low-concentration ammonia in ambient air.~~

~~3.1~~3.2 Setting reaction conditions

However, ~~But for on-line instruments,~~ precipitates can attach to the wall of the pipeline and LWCC for on-line instruments, which leads to pipeline blockage and baseline drift. Therefore, we need to optimize reaction conditions, add the constant temperature module and liquid flow controller temperature~~, and so on~~ to achieve continuous online measurement of low-concentration ammonia in ambient air.

The concentration of the R1 we used in the initial reaction conditions (longer optical path and smaller sampling volume) ~~The stripping solution~~ contained 1 g L^{-1} salicylic acid ~~$C_6H_4(OH)(COOH)$~~, 0.1 g L^{-1} sodium nitroprussides ~~$Na_2[Fe(CN)_5NO]^{2-}$~~, and 1 g L^{-1} NaOH. 0.5 ml L^{-1} sodium hypochlorite ~~NaClO~~and 3 g L^{-1} NaOH were used as ~~derivatization solution~~ R2 ~~based on the former scholar (Krom and Michael, 1980; Searle and Phillip, 1984),~~(Krom and Michael, 1980; Searle and Phillip, 1984). ~~and the state of our experiment status (Longer optical path and lower sampling volume) in the initial reaction condition.~~ In addition, ~~particulate matter filter~~ the syringe filter was introduced to ~~, which could~~ minimize the influence of precipitate ~~sediment~~ (Bianchi et al., 2012), but a large ~~deviation~~ drift of the baseline would still occur during the long time run in our experiment, which will be discussed in detail later. In fact, we tried interrupting the sampling for a few minutes and implementing 5% hydrochloric acid for the system to remove these precipitates. However, the concentration changed greatly before and after each cleaning precipitation. In addition, once the precipitation was formed, it will take a long time to remove the precipitation, which will also increase the risk of contaminating the detector. According to reaction kinetics, reducing the stripping and derivatization concentrations (solution concentration) ~~solution concentration~~ and [OH^-] of the system can greatly reduce the formation of precipitates in the solution. Therefore, we need to find the optimal reaction conditions to produce the least amount of precipitate. The maximum absorbance of a 100 μg L^{-1} NH_4^+ standard solution was obtained at 18.75 mmol L^{-1} OH^- and we could obtain ~~As shown in Figure 3, higher [OH^-] leaded to a lower voltage signal and higher absorbance, but the effect was no longer apparent when [OH^-] increased to 18.75 mmol L^{-1}.~~

~~We chose an 18.75 mmol L^{-1} OH^- solution system with the aim of obtaining~~ a high absorbance of light and a slow speed of precipitate formation, which meant that 1.5 g L^{-1} NaOH was added to the derivatization solution~~. And in this study, the stripping solution was prepared by dissolving 0.75 g L^{-1} $C_6H_4(OH)(COOH)$ (TCI, 99.5%, Japan), 0.014 g L^{-1} $Na_2[Fe(CN)_5NO]^{2-}$ (TCI, 99%, Japan), and 0.2 g L^{-1} NaOH. For the derivatization solution, 0.188 ml L^{-1} NaClO (Aladdin, active chlorine10%, China) and 1.5 g L^{-1} NaOH~~, ~~which~~ resulted in the precipitate in the solution being too small to cause pipeline blockage and baseline drift. Importantly, we added regular assessment of the system drift through use of online sampling of pure N_2. The range of blank signal in continuous operation for 48 h were 2.856 V ~ 2.848 V and 2.254 V ~ 1.834 V of reduced solution concentration and former high solution concentration, and the maximum offset were 0.3% and 18.6%, respectively, the baseline of low concentration solution has better stability (Fig. 3). In addition, ~~Importantly,~~ the concentrations of salicylic acid~~$C_6H_4(OH)(COOH)$~~, sodium nitroferricyanide ~~$Na_2[Fe(CN)_5NO]^{2-}$~~ and sodium hypochlorite ~~NaClO~~ were~~ 96 %, 98 %, and 99 % lower~~ 0.04, 0.02 and 0.006 times lower than those in previous research, respectively (Bianchi et al., 2012).

In ~~other words~~general, the iron-containing precipitate increase the absorbance by scattering or absorbing light, resulting in measurement bias. In this study, the amount of iron-containing precipitation is very small by reducing the content of components and alkali of the solution system, and the voltage of the instrument will not drop significantly due to contamination, which is conducive to better maintenance of the baseline~~ (Fig. 4)~~.

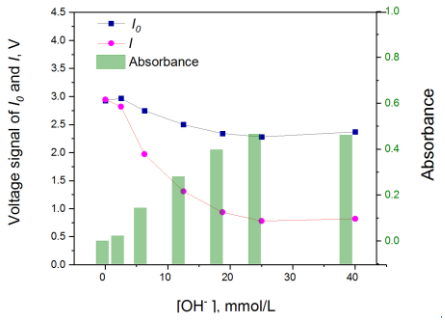

~~Fig. 3. The influence of [OH^-] on the voltage signal and absorbance~~

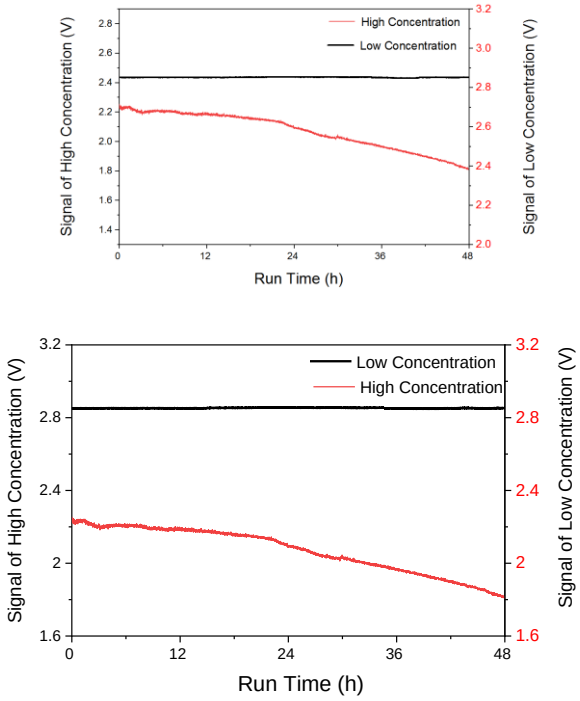

域代码已更改

Fig. ~~5~~3. The blank time series of the NH_3 detector ran continuously for ~~72~~ 48 h.(Low concentration: 0.75g L^{-1} salicylic acid, 0.014 g L^{-1} sodium nitroferricyanide, and 0.2 g L^{-1} NaOH as R1, then the 0.188ml L^{-1} Sodium hypochlorite and 1.5 g L^{-1} NaOH as R2; High concentration: 1g L^{-1} salicylic acid, 0.1 g L^{-1} sodium nitroferricyanide, and 1 g L^{-1} NaOH as R1, then the 0.5ml L^{-1} Sodium hypochlorite and 3 g L^{-1} NaOH as R2).

3.3 Stability of liquid flow and temperature

The temperature control module and flow control system were designed because of the sensitivity of molecular absorption spectrophotometry to ambient temperature and residence time. A commercial PID temperature controller was used to control the temperature of the reaction ~~kettle~~ coil with the accuracy of ±0.1 ℃. The temperature control module was used to control the constant temperature from the reaction ~~kettle~~ coil to LWCC at 55.0±0.1 ℃. At the same time, the flow control system could control the rotational speed of the peristaltic. This system used a commercialized liquid flow meter (SLI-1000, Sensirion, Switzerland)~~new type of photoelectric detection to bubbly flow, which could~~ detect the flow

rate and feedback to the peristaltic pump control by detecting the flow of tiny bubbles, which further improved the stability of the reaction process. In other words, the flow control system could avoid the flow rate dropping caused by the abrasion of the pump tube and ~~the bump up of~~ increase the flow rate caused by the replacement of the pump tube, keeping the ~~stripping solution~~R1 flow at a constant set point (0.49 ml min^{-1}).

In addition, we designed a buffer tube with a cooling function to further reduce the effects of precipitation. After the derivatization reaction in the reaction coil at 55.0 ℃~~A chromogenicreaction in the reaction kettle at 55.0 ℃~~, the mixed solution entered the cooling buffer tube. Most of the precipitation was generated in the buffer tube and attached to the tube wall, while some of the precipitation generated in the downstream pipeline was intercepted by an in-line precipitate filter with a pore size of 1.0 μm before the LWCC.

Overall, the above work can make the instrument maintain a relatively stable reaction time and temperature, which can promote a relatively stable reaction process, resulting in a high reproducibility to the same concentration of NH_3~~NH_4^+~~. In the calibration process, R1 was used as diluent, and the concentrations were 10, 25, 50, 75, 100, 150, and 200μg L^{-1} of NH_4^+ standard solution. High purity N_2 was used as blank gas into the sampling tube, and the standard solution entered the solution system instead of the R1~~1~~. F~~F~~ig. ~~6~~ 4 showed the calibration with the NH_4^+ concentration gradient of ~~0~~ 100~~0~~, 10, 25, 50 and 100 μg L^{-1} (150, and 200μg L^{-1} of NH_4^+ standard solutions were out of the detection range, which was discussed in section 3.4). Each concentration point was run for 40 minutes, and the ~~relative standard deviations~~RSD calculated from four consecutive measurements (the collection of the four replicates were completed during a 4-week of constant instrument operation) ~~–~~ranged from 0.32 % to 2.65 ~~%.~~ %, with the k varying from 0.0037 to 0.0040. Moreover, the blank experiment tests were automatically made every one or two days, that is, high purity N_2 was used as a blank gas through the sample tube for 40 minutes, the RSD of the blank signal in continuous operation for one month ~~(blank tests were made every one or two days)~~ was 1.8 %, which indicated good repeatability and stability of the instrument. ~~showing good stability.~~ Seven switching samples were performed with 50 μg L^{-1} NH_4^+ standard solution and R1, ~~After~~ after calculating 10-90 % of the full signal after a change in concentration, the time response ~~resolution~~ was approximately 140 s, which was much quicker than the method described by Bianchi et.al (measured to be 10 min) (Bianchi et al., 2012).

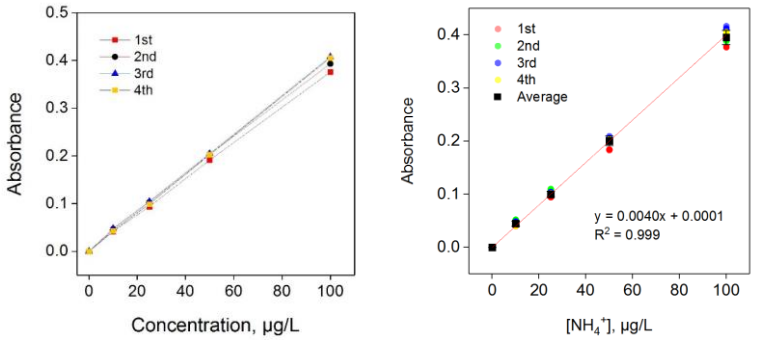

Fig. 4. Calibration curves of standard solution with the same concentration gradient 4 times

Table 1. Linear regression with the same concentration gradient 4 times

Time	k	b	R^2
1st	0.0037	0.0018	0.9998
2nd	0.0039	0.0046	0.9996
3rd	0.0040	0.0034	0.9997
4th	0.0040	0.0003	0.9999

~~Number~~		~~0 μg L^{-1} solution (μg L^{-1})~~	~~Response of standard solutions (μg L^{-1})~~
~~1~~		~~-0.014~~	~~49.529~~
~~2~~		~~-0.082~~	~~49.615~~
~~3~~		~~-0.014~~	~~50.773~~
~~4~~		~~0.019~~	~~50.599~~
~~5~~		~~0.053~~	~~50.019~~
~~6~~		~~0.086~~	~~50.019~~
~~7~~		~~-0.048~~	~~49.443~~
	~~AVG~~	~~0.000~~	~~50.000~~
	~~STD~~	~~0.053~~	~~0.484~~
	~~RSD~~		~~0.97%~~

~~3~~3.4.~~3~~ Setup of the temperature

~~However, the reduction of the content of components in the solution will lead to a decrease in absorbance, so it is necessary to adjust the temperature to speed up the reaction process and achieve a higher absorbance.~~

High temperature can accelerate the reaction process and achieve better measurement accuracy and precision. ~~As shown in Figure 5a, t~~The voltage signal decreased with increasing temperature; conversely, the absorbance increased with temperature. According to the flow rate (gas flow rate of 0.70 L min^{-1}, liquid flow rate of 0.49 ml min^{-1}), the detection limit of our SAC-LOPAP can reduce to less than 50 ppt when the absorbance of 50 μg L^{-1} NH_4^+ standard solution reached 0.15 or more. However, if the temperature is too high, there is a danger that the pipeline interface of the instrument will fall off. Considering the continuous delivery of solutions (the stability of pipeline connections) and the detection limit (lower than 50 ppt) ~~Considering the stability and detection range of the instrument~~, 55 ℃ was selected as the best reaction operating temperature of the instrument, at which sufficient absorbance could be achieved to detect ~~low~~ concentrations of ammonia gas.

~~Furthermore,~~ The standard solution entered the solution system instead of the stripping solution, then the measured absorbance values were used as absorbance-standard solution concentration plot and regression calculation (The experimental process has been described in Section 3.3). The result is shown in Fig. 5, a high degree of correlation was found between the standard solution and absorbance with a correlation coefficient of R^2 = 0.99 for the standard solution of 0-~~100~~ 100 μg L^{-1} ~~(Fig. 5)~~, however, due to the incomplete reaction of NH_4^+ with dye products, there are two points outside of the linear fit (standard solution concentrations are 150 and 200 μg L^{-1}). Therefore, the approximate mixing ratio of NH_3 corresponding to the standard liquid concentration is 0-99.1 ppb, which is more than adequate for monitoring urban areas. The detection limit for NH_4^+ liquid solution is about 40.9 ng L^{-1}, which is calculated as 3 times the average standard deviation of blank signal noise in one hour. With an air sample flow rate of 0.7 L min^{-1} and a liquid flow rate of 0.49 ml min^{-1}, this translates to a gas phase mixing ratio of about 40.5 ppt. ~~indicating that the measurement range was background contamination up to 100 μg L^{-1} for NH_4^+ solutions. Under the above reaction conditions and temperatures, the detection limit of NH_3 was 40.5 ppt (gas flow rate of 0.70 L min^{-1}, liquid flow rate of 0.49 ml min^{-1}),~~In other words, ~~–~~ the

measurement range was 40.5 ppt up to ~~100~~ 99.1 ppb for NH_3, which was well suited for the investigation of the NH_3 budget from urban to rural conditions in China. At the same time, ~~A~~according to the zero point data and the calibration, the corresponding concentration to the voltage signal of 0.1 mV is 3.1 ppt, which far meets our requirements for actual environmental measurement.

Importantly, the detection limit can be decreased by improving the gas flow. We can increase our detection range by reducing the reaction temperature and shortening the length of LWCC. When the temperature drops to 50 ℃, the range can be up to 200 ppb.

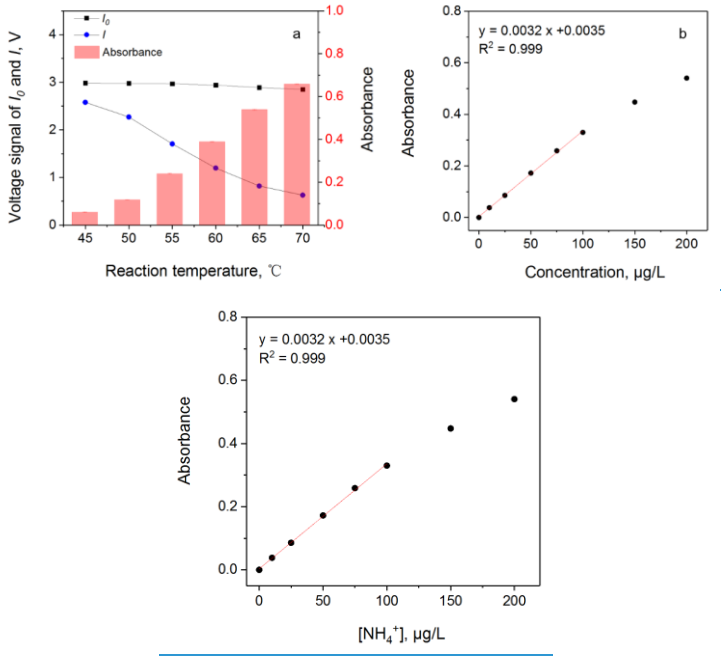

Fig. 5. Standard solution and absorbance liner range test, to get a measurement range

4. Comparison in urban Beijing

~~The field campaign of SAC-LOPAP was conducted at the College of Environment Sciences and Engineering, Peking University, located within the 4th ring road in northern Beijing (40 ° N, 116 ° E), China. A commercial instrument Picarro G2103 analyzer (Picarro, US) used for atmospheric NH_3 measurement based on the CRDS method was deployed concurrently with SAC-LOPAP in the field~~

带格式的: 缩进: 首行缩进: 0 厘米

~~comparison, which could be used to calibrate and validate other instruments (Twigg et al., 2022). The inter-comparison experiment took place from 15 September 2021 to 15 October 2021, with the instruments installed in a field container. Two instruments were deployed with a common inlet height of 2.5 m above the ground. The inlet tube was a 3.8 m long 1/4′ Teflon tube covered with thermo-isolation materials. Additionally, we removed the particles with a Teflon filter at the front of the sampling inlet and changed the filter every day with the aim of avoiding uncertainties. Data acquisition times were different for the above instruments during the inter-comparison. The base reporting periods for Picarro and SAC-LOPAP were 1 s and 30 s. For the purposes of comparison, data from the two instruments presented in this section were averaged to 5 min. In addition, zero point was carried out every 7 days, and the standard gas was usually introduced into the instruments 40 min after zero gas so that they could maintain stability in the measurement process and ensured quality control.~~

The time series of the concentration of NH_3 during the inter-comparison period of Picarro and SAC-LOPAP were presented in Fig. ~~7a~~6a. There were a few data gaps for the above instruments caused by calibration operations and instrument maintenance. Instruments display similar temporal features for NH_3 concentrations over the duration of the study. In this study, the concentration of our instrument ranged from 1.3 ppb to 47.86 ppb with an average of 12.64 ± 8.63 ppb, which was close to the concentrations of Picarro (12.76 ± 8.57 ppb). The response speed was similar, indicated that SAC-LOPAP responded in time to rapid changed in NH_3 concentration. The diurnal variation results showed that the concentrations measured by the two instruments were very similar, with our instrument slightly lower than Picarro by 0.72 ppb (Fig. 6b). ~~Fig.7b and Fig.7c showed that the two instruments had a deviation in response to the peak formed by the rapid rise and fall of NH_3 concentration, which might be caused by the blank deviation between both instruments. Still, the response speed was similar, indicated that SAC-LOPAP responded in time to rapid changed in NH_3 concentration at the five-minute resolution.~~ Furthermore, relatively good correlations for the NH_3 data observed by these instruments were achieved over a large dynamic range of concentration with a slope of 1.00 and an R^2 of 0.96 (Fig. ~~7a~~6c). We found that most of the time there were good correlations between the two instruments within one day except for the data of 23th and 30th September. The regression slope for all the days with higher and lower slopes are 1.46 and 0.72, respectively. We performed in-situ testing of both systems with a cylinder, we produced NH_3 concentrations of about 1.32, 4.95, 9.59, 17.90 and 54.96 ppb. Fig. 6d showed regression

analyses of the NH_3 standard gas concentrations obtained with the two instruments. The NH_3 concentrations measured by picarro and our instrument were strongly correlated, with a slope of 1.01 and an R^2 of 0.99.

~~The NH_3 concentrations measured by those instruments were strongly correlated (R^2 = 0.967), which significantly indicated that the SAC-LOPAP developed in this study could measure the NH_3 concentration accurately.~~ In general, our instrument run relatively stable with the ~~STD~~ standard deviation of zero gas during the one month of observations being within 26 ppt (Picarro: 23 ppt), which was far below our detection limit. ~~and both systems agreed for the RSD of the standard gas within 0.76 % (Table 2),~~ Furthermore, the drift of SAC-LOPAP and Picarro at 4.95 ppb were 3.5% and 2.8%, while the drifts of 54.96 ppb were 1.5% and 0.7%, which meant that our instrument could keep steady for a long time and it could be used for the continuous online measurement of low concentration of ambient air. More detailed inter-comparison for these NH_3 instruments will be analyzed in a future publication.

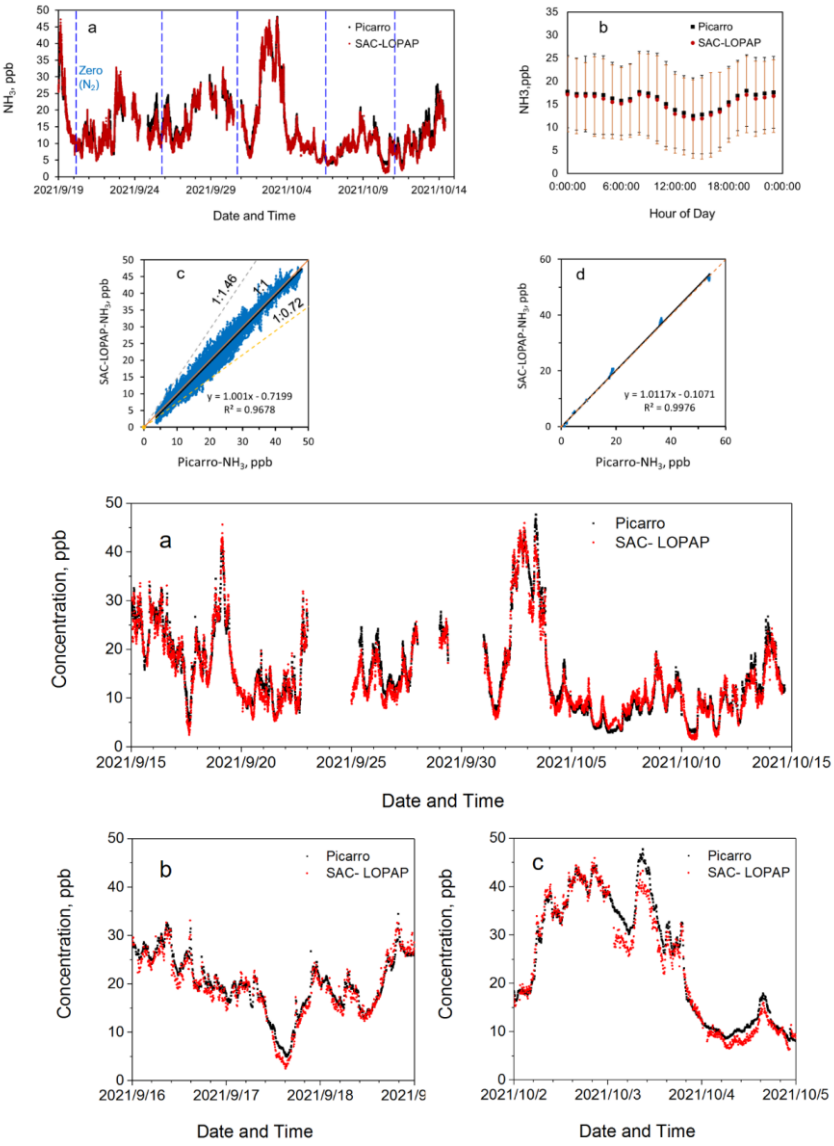

Fig. 6. (a) Time series of NH_3 concentration during the comparison, (b) Diurnal variation of NH_3 concentrations observed by Picarro and SAC-LOPAP, (c) Regression analysis of the NH_3 concentrations observed by Picarro and

SAC-LOPAP, and (d) Regression analysis of different concentrations of Picarro and SAC-LOPAP NH_3 standard gases.

~~Fig. 7. (a) Time series of NH_3 concentration during the field comparison, and (b), (c) Magnified view of time series.~~

~~Table 2. Reproducibility test by zero gas and standard gas~~

~~Test number~~	~~Zero gas (ppb)~~		~~NH_3 standard (ppb)~~	
	~~SAC-LOPAP~~	~~Picarro~~	~~SAC-LOPAP~~	~~Picarro~~
~~1~~	~~0.014~~	~~0.856~~	~~40.732~~	~~40.291~~
~~2~~	~~0.074~~	~~0.898~~	~~40.221~~	~~40.072~~
~~3~~	~~0.069~~	~~0.859~~	~~40.710~~	~~39.995~~
~~4~~	~~0.031~~	~~0.908~~	~~40.022~~	~~40.011~~
~~5~~	~~0.062~~	~~0.876~~	~~40.373~~	~~40.076~~

5. Conclusions

Ammonia (NH_3) in the atmosphere affects the environment and human health and is therefore increasingly recognized by policy makers as an important air pollutant that needs to be mitigated. The accurate and precise detection of ambient NH_3 concentrations is therefore an urgent need for the exploration of secondary pollution at the regional scale in China.

At the present stage, ambient NH_3 measurements at many supersites are still done with spectroscopic, mass spectrometric and wet chemical methods, which are restricted by the high detection limit and lower time resolution. In this study, we provide an online NH_3 monitoring system based on wet chemistry stripping and long path absorption photometer of atmospheric NH_3, our new SAC-LOPAP system has several significant improvements: one is the~~We improved on-line monitoring technology to measure NH_3 in the atmosphere, which had been used for continuous on-line measurement of low concentration ambient air for a long time. Our SAC-LOPAP is a combination of the Berthelot reaction and long path absorption photometer for gaseous ammonia measurement. It has several notable improvements compared to previous setups, as reported by other studies, and one is the~~ optimization of reaction conditions. The low concentration but higher flow rate of solutions decreases the precipitate's production, and the cooling buffer tube and the filter trap most of the precipitates. The others are the constant temperature module and liquid flow controller. The constant temperature module in the system reduces

带格式的: 字体: (中文) 宋体, 字体颜色: 文字 1

带格式的: 左

the influence of ambient temperature on the reaction process and color degree. Similarly, adding a liquid flow controller is helpful to the stability of the flow rate and further increases the stability of the reaction process. These improvements reduce the system error and significantly increase the sustainability of SAC-LOPAP operation. Our instrument reached a detection limit of about 40.5 ppt with a stripping liquid flow rate of 0.49 ml min^{-1} and a gas sample flow rate of 0.70 L min^{-1} in the current condition, and the measuring range of the instrument is 0-99.1 ppb. Our system has also been characterized in a laboratory setting where we can measure low concentrations. SAC-LOPAP and Picarro were compared in urban areas for a month ~~–~~with relatively good agreement (R^2 = 0.967). In addition, the diurnal variation results showed that the concentrations of the two instruments were very similar.~~The detection limit reached with this instrument is 40.5 ppt under stable conditions. The range of NH_3 measurement vary from background contamination (<40.5 ppt) to approximately 100 ppb with a stripping liquid flow rate of 0.49 ml min^{-1} and a gas sample flow rate of 0.70 L min^{-1} in the current condition. SAC-LOPAP had a STD of zero point signal within 26 ppt, also agreed for the RSD of the standard gas within 0.76 % within a month, which indicating that the instrument could run statically for a long time and the repeatability was g Tood.~~ ~~T~~herefore, we conclude that our update of the ammonia measurement experimental framework has been successful. However, more research about field measurement and comparison is needed to verify the equipment's performance in routine observation, and the influence of particulate ammonium on the results of NH_3 detection also requires further study.

Data availability. The datasets used in this study are available from the corresponding author upon request (hbdong@pku.edu.cn).

Author contributions. H.B.D. designed the study. S.S.T., K.X.Z. set up and characterized the instrument, analyzed the data and wrote the paper with the input of H.B.D. As co-authors, S.S.T and K.X.Z. contributed equally to this paper. All authors contributed to the field measurements, discussed and improved the paper.

Competing interests. The authors declare that they have no conflict of interest.

Acknowledgments. This work was supported by special fund of State Key Joint Laboratory of Environmental Simulation and Pollution Control (Grants No.22Y04ESPCP)

References.

Ajay and Beniwal.: Electrospun SnO2/PPy nanocomposite for ultra-low ammonia concentration detection at room temperature, Sensors & Actuators B Chemical, 296, 126660.126661-126660.126669, https://doi.org/10.1016/j.snb.2019.126660, 2019.

Bae, M. S., Demerjian, K. L., Schwab, J. J., Weimer, S., Hou, J., Zhou, X., Rhoads, K., and Orsini, D.: Intercomparison of Real Time Ammonium Measurements at Urban and Rural Locations in New York, Aerosol Science & Technology, 41, 329-341, https://doi.org/10.1080/02786820701199710, 2007.

Baek, B. H. and Aneja, V. P.: Measurement and analysis of the relationship between ammonia, acid gases, and fine particles in eastern North Carolina, Air Repair, 54, 623-633, https://doi.org/10.1080/10473289.2004.10470933, 2004.

Behera, S. N., Sharma, M., Aneja, V. P., and Balasubramanian, R.: Ammonia in the atmosphere: a review on emission sources, atmospheric chemistry and deposition on terrestrial bodies, Environ Sci Pollut Res Int, 20, 8092-8131, https://doi.org/10.1007/s11356-013-2051-9 2013.

Benson, D. R., Markovich, A., Al-Refai, M., and Lee, S. H.: A Chemical Ionization Mass Spectrometer for ambient measurements of Ammonia, Atmos. Meas. Tech., 3, 1075-1087, https://doi.org/10.5194/amt-3-1075-2010, 2010.

526 Berden, G., Peeters, R., Meijer, G., and Apituley, A.: Open-path trace gas detection of ammonia
527 based on cavity-enhanced absorption spectroscopy, Applied Physics B 71, 231-216,
528 https://doi.org/10.1007/s003400000302, 2000.
529 Bessagnet, B., Beauchamp, M., Guerreiro, C., Leeuw, F. D., Tsyro, S., Colette, A., Meleux, F., Rou?L,
530 L., Ruyssenaars, P., and Sauter, F.: Can further mitigation of ammonia emissions reduce
531 exceedances of particulate matter air quality standards?, Environmental Science & Policy, 44,
532 149-163, https://doi.org/10.1016/j.envsci.2014.07.011, 2014.
533 Bianchi, F., Dommen, J., Mathot, S., and Baltensperger, U.: On-line determination of ammonia at
534 low pptv mixing ratios in the CLOUD chamber, Atmospheric Measurement Techniques,5,7(2012-
535 07-19), 5, 1719-1725, https://doi.org/10.5194/amt-5-1719-2012, 2012.
536 Callahan, M. R., Rose, J. B., and Byrne, R. H.: Long pathlength absorbance spectroscopy: trace
537 copper analysis using a 4.4 m liquid core waveguide, Talanta, 58, 891-898,
538 https://doi.org/10.1016/S0039-9140(02)00403-4 2002.
539 Chen, X., Oro, Y., Tanaka, K., Takenaka, N., and Bandow, H.: A New Method for Atmospheric
540 Nitrogen Dioxide Measurements Using the Combination of a Stripping Coil and Fluorescence
541 Detection, Analytical Sciences the International Journal of the Japan Society for Analytical
542 Chemistry, 20, 1019-1023, https://doi.org/10.2116/analsci.20.1019, 2004.
543 Dong, H. B., Zeng, L. M., Hu, M., Wu, Y. S., Zhang, Y. H., Slanina, J., Zheng, M., Wang, Z. F., and
544 Jansen, R.: Technical Note: The application of an improved gas and aerosol collector for ambient
545 air pollutants in China, ATMOSPHERIC CHEMISTRY AND PHYSICS, 12, 10519-10533,
546 https://doi.org/10.5194/acp-12-10519-2012, 2012.
547 Fowler, D., Steadman, C. E., Stevenson, D., Coyle, M., Rees, R. M., Skiba, U. M., Sutton, M. A.,
548 Cape, J. N., Dore, A. J., and Vieno, M.: Effects of global change during the 21st century on the
549 nitrogen cycle, Atmospheric chemistry and physics, 15, 13849-13893,
550 https://doi.org/10.5194/acp-15-13849-2015, 2015.
551 Gong, D., Liucheng, L. I., Baozeng, L. I., Liping, D., Wang, Y., Yanhua, M. A., Zhang, Z., and Jin, Y.:
552 NH3 measurement based on cavity enhanced absorption spectroscopy, Laser Technology, 5,
553 664-668, https://doi.org/10.7510/jgjs.issn.1001-3806.2017.05.009, 2017.
554 Heland, J., Kleffmann, J., Kurtenbach, R., and Wiesen, P.: A new instrument to measure gaseous
555 nitrous acid (HONO) in the atmosphere, Environmental Science & Technology, 35, 3207-3212,
556 2001.
557 Hüglin, E.: Ammonia monitoring at trace level using photoacoustic spectroscopy in industrial and
558 environmental applications, Spectrochimica Acta Part A: Molecular and Biomolecular
559 Spectroscopy, 60, 3259-3268, https://doi.org/10.1016/j.saa.2003.11.032, 2004.
560 Ianniello, A., Spataro, F., Esposito, G., Allegrini, I., Hu, M., and Zhu, T.: Chemical characteristics of
561 inorganic ammonium salts in PM2.5 in the atmosphere of Beijing (China), Atmospheric Chemistry
562 & Physics, 11, 10803-10822, https://doi.org/10.5194/acp-11-10803-2011, 2011.
563 Janson, R., Rosman, K., Karlsson, A., and H.-C.HANSSON: Biogenic emissions and gaseous
564 precursors to forest aerosols, Tellus, 53, 423-440, https://doi.org/10.1034/j.1600-0889.2001.d01-
565 30.x, 2010.
566 Khlystov, A., Wyers, G. P., Brink, H., and Slanina, J.: The steam-jet aerosol collector (SJAC), Journal
567 of Aerosol Science, 26, S111-S112, https://doi.org/10.1016/0021-8502(95)96963-8 1995.

Kleffmann, J., Heland, J., Kurtenbach, R., Lrzer, J. C., and Wiesen, P.: A new instrument (LOPAP) for the detection of nitrous acid (HONO), Environmental Science and Pollution Research, 9, 48-54, 2002.
Klimczyk, M., Siczek, A., and Schimmelpfennig, L.: Improving the efficiency of urea-based fertilization leading to reduction in ammonia emission, Science of The Total Environment, 771, 145483, https://doi.org/10.1016/j.scitotenv.2021.145483, 2021.
Krom and Michael, D.: Spectrophotometric determination of ammonia: a study of a modified Berthelot reaction using salicylate and dichloroisocyanurate, Analyst, 105, 305-316, https://doi.org/10.1039/an9800500305, 1980.
Krupa, S. V.: Effects of atmospheric ammonia (NH3) on terrestrial vegetation: a review, Environmental Pollution, 124, 179-221, https://doi.org/10.1016/S0269-7491(02)00434-7 2003.
Makkonen, U., Virkkula, A., Mantykentta, J., Hakola, H., Keronen, P., Vakkari, V., and Aalto, P. P.: Semi-continuous gas and inorganic aerosol measurements at a Finnish urban site: comparisons with filters, nitrogen in aerosol and gas phases, and aerosol acidity, Atmospheric Chemistry and Physics, 12, 5617-5631, https://doi.org/10.5194/acp-12-5617-2012, 2012.
Martin, N. A., Ferracci, V., Cassidy, N., and Hoffnagle, J. A.: The application of a cavity ring-down spectrometer to measurements of ambient ammonia using traceable primary standard gas mixtures, Applied Physics B, 122, 219, https://doi.org/10.1007/s00340-016-6486-9, 2016.
Mcmanus, J. B., Nelson, D. D., Shorter, J. H., Zahniser, M. S., and Faist, J.: Quantum cascade lasers for open- and closed-path measurement of trace gases, Society of Photo-Optical Instrumentation Engineers (SPIE) Conference Series, 4817, https://doi.org/10.1117/12.452093 2002.
Ni, Ji-Qin, Heber, Albert, J., Lim, Teng, T., Diehl, and Claude: Ammonia Emission from a Large Mechanically-Ventilated Swine Building during Warm Weather, Journal of Environment Quality, 29, 751-751, https://doi.org/10.2134/jeq2000.00472425002900030010x, 2000.
Nowak, J. B., Neuman, J. A., Kozai, K., Huey, L. G., Tanner, D. J., Holloway, J. S., Ryerson, T. B., Frost, G. J., McKeen, S. A., and Fehsenfeld, F. C.: A chemical ionization mass spectrometry technique for airborne measurements of ammonia, Journal of Geophysical Research-Atmospheres, 112, https://doi.org/10.1029/2006jd007589, 2007.
Qu, Z. C., Li, B. C., and Han, Y. L.: Cavity ring-down spectroscopy for trace ammonia detection, Journal of Infrared & Millimeter Waves, 31, 431-436, https://doi.org/10.3724/SP.J.1010.2012.00431, 2012.
Scab, C., Mc, D., Zheng, G. E., Wen, X. F., Xdd, G., and Yu, L.: Enhanced atmospheric ammonia (NH3) pollution in China from 2008 to 2016: Evidence from a combination of observations and emissions - ScienceDirect, Environmental Pollution, 263, https://doi.org/10.1016/j.envpol.2020.114421, 2020.
Searle and Phillip, L.: The berthelot or indophenol reaction and its use in the analytical chemistry of nitrogen. A review, Analyst, 109, 549-540, 1984.
Sharma, S. K., Datta, A., Saud, T., Saxena, M., Mandal, T. K., Ahammed, Y. N., and Arya, B. C.: Seasonal variability of ambient NH3, NO, NO2 and SO2 over Delhi, Journal of Environmental Sciences, 22, 1023-1028, https://doi.org/10.1016/S1001-0742(09)60213-8 2010.

609 Sharma, S. K., Singh, A. K., Saud, T., Mandal, T. K., Saxena, M., Singh, S., Ghosh, S. K., and Raha, S.:
610 Measurement of ambient NH3 over Bay of Bengal during W_ICARB Campaign, Annales
611 Geophysicae, 30, 371-377, https://doi.org/10.5194/angeo-30-371-2012, 2012.
612 Sutton, M. A., Fowler, D., Burkhardt, J. K., and Milford, C.: Vegetation atmosphere exchange of
613 ammonia: canopy cycling and the impacts of elevated nitrogen inputs, Water Air & Soil Pollution,
614 85, 2057-2063, https://doi.org/10.1007/BF01186137 1995.
615 Swati, A. and Hait, S.: Greenhouse Gas Emission During Composting and Vermicomposting of
616 Organic Wastes – A Review, CLEAN - Soil Air Water, 46, 1700042.1700041-1700042.1700013,
617 https://doi.org/10.1002/clen.201700042, 2018.
618 Twigg, M. M., Berkhout, A. J. C., Cowan, N., Crunaire, S., Dammers, E., Ebert, V., Gaudion, V.,
619 Haaima, M., Häni, C., John, L., Jones, M. R., Kamps, B., Kentisbeer, J., Kupper, T., Leeson, S. R.,
620 Leuenberger, D., Lüttschwager, N. O. B., Makkonen, U., Martin, N. A., Missler, D., Mounsor, D.,
621 Neftel, A., Nelson, C., Nemitz, E., Oudwater, R., Pascale, C., Petit, J. E., Pogany, A., Redon, N.,
622 Sintermann, J., Stephens, A., Sutton, M. A., Tang, Y. S., Zijlmans, R., Braban, C. F., and
623 Niederhauser, B.: Intercomparison of in situ measurements of ambient NH3: instrument
624 performance and application under field conditions, Atmos. Meas. Tech., 15, 6755-6787,
625 https://doi.org/10.5194/amt-15-6755-2022, 2022.
626 Von, B. K., Braban, C. F., Famulari, D., Jones, S. K., Blackall, T., Smith, T., Blom, M., Coe, H.,
627 Gallagher, M., and Ghalaieny, M.: Field inter-comparison of eleven atmospheric ammonia
628 measurement techniques, Atmospheric Measurement Techniques, 3, 91-112,
629 https://doi.org/10.5194/amt-3-91-2010, 2009.
630 Wang, Ruyu, Ye, Xingnan, Liu, Yuxuan, Li, Haowen, Yang, and Xin: Characteristics of atmospheric
631 ammonia and its relationship with vehicle emissions in a megacity in China, Atmospheric
632 Environment, 182, 97-104, https://doi.org/10.1016/j.atmosenv.2018.03.047, 2018.
633 Wang, S., Nan, J., Shi, C., Fu, Q., Gao, S., Wang, D., Cui, H., Saiz-Lopez, A., and Zhou, B.:
634 Atmospheric ammonia and its impacts on regional air quality over the megacity of Shanghai,
635 China, Scientific Reports, 5, 15842, https://doi.org/10.1038/srep15842, 2015.
636 Wang, Y., Zhang, Q. Q., He, K., Zhang, Q., and Chai, L.: Sulfate-nitrate-ammonium aerosols over
637 China: response to 2000–2015 emission changes of sulfur dioxide, nitrogen oxides, and
638 ammonia, Atmospheric Chemistry and Physics, 13, 2635-2652 https://doi.org/10.5194/acp-13-
639 2635-2013, 2013.
640 Wen, Liang, Xue, Likun, Wang, Xinfeng, Xu, Caihong, Chen, and Tianshu: Summertime fine
641 particulate nitrate pollution in the North China Plain: increasing trends, formation mechanisms
642 and implications for control policy, Atmospheric Chemistry & Physics, 18, 11261-11275,
643 https://doi.org/10.5194/acp-2018-89, 2018.
644 Whitehead, J. D., Twigg, M., Famulari, D., Nemitz, E., Sutton, M. A., Gallagher, M. W., and Fowler,
645 D.: Evaluation of Laser Absorption Spectroscope Techniques for Eddy Covariance Flux
646 Measurements of Ammonia, Environmental Science & Technology, 42, 2041-2046,
647 https://doi.org/10.1021/es071596u, 2008.
648 Yao, W., Byrne, R. H., and Waterbury, R. D.: Determination of Nanomolar Concentrations of
649 Nitrite and Nitrate in Natural Waters Using Long Path Length Absorbance Spectroscopy,
650 Environmental Science and Technology, 32, 2646-2649, https://doi.org/10.1021/es9709583
651 1998.

652 Yokelson and R., J.: Evaluation of adsorption effects on measurements of ammonia, acetic acid,
653 and methanol, Journal of Geophysical Research Atmospheres, 108, -, 2003.
654 Yokelson, R., Christian, T., Bertschi, I., and Hao, W.: Evaluation of adsorption effects on
655 measurements of ammonia, acetic acid, and methanol, Journal of Geophysical Research
656 Atmospheres, 108, https://doi.org/10.1029/2003JD003549, 2003.
657 Yu, H. and Lee, S. H.: Chemical ionisation mass spectrometry for the measurement of
658 atmospheric amines, Environmental Chemistry, 9, 190-201,
659 https://doi.org/10.1029/2003JD00354910.1071/en12020, 2012.

660